# SCIENCE CHINA

# Physics, Mechanics & Astronomy



• Article • SPECIAL TOPIC:

xxx 2025 Vol. xx No. x: 0000000 https://doi.org/xx

# A stringent constraint on the fractional change of proton g-factor

Renzhi Su\*†1,2, Stephen, J., Curran\*3, Jeremy Darling<sup>4</sup>, Minfeng Gu<sup>1</sup>, J. N. H. S. Aditya<sup>5,6</sup>, Ningyu Tang<sup>7</sup>, Di Li<sup>8,9</sup>, and Zheng Zheng<sup>9</sup>

Shanghai Astronomical Observatory, Chinese Academy of Sciences, 80 Nandan Road, Shanghai 200030, China;
 Research Center for Astronomical Computing, Zhejiang Laboratory, Hangzhou 311100, China;
 School of Chemical and Physical Sciences, Victoria University of Wellington, PO Box 600, Wellington 6140, New Zealand;
 Centre for Astrophysics and Space Astronomy, Department of Astrophysical and Planetary Sciences, University of Colorado, 389 UCB, Boulder, CO 80309-0389, USA;
 Sydney Institute for Astronomy, School of Physics A28, University of Sydney, NSW 2006, Australia;
 ARC Centre of Excellence for All Sky Astrophysics in 3 Dimensions (ASTRO 3D), Sydney, Australia;
 Department of Physics, Anhui Normal University, Wuhu, Anhui 241002, People's Republic of China;
 New Cornerstone Science Laboratory, Department of Astronomy, Tsinghua University, Beijing 100084, China;

<sup>9</sup>National Astronomical Observatories, Chinese Academy of Sciences, Beijing 100012, China

Received xx; accepted xx

We report a constraint on the cosmological variation of the proton g-factor,  $g_p$ . By comparing the measured redshifts between H  $_1$  21 cm and OH 18 cm lines observed with the newly commissioned Five-hundred-meter Aperture Spherical radio Telescope (FAST) toward PKS 1413+135 at z=0.24671, we obtain  $\Delta g_p/g_p=(-4.3\pm2.5)\times10^{-5}$ , which is more than two orders of magnitude more sensitive than previous constraints. In addition, we obtain sensitive constraints of  $\Delta(\mu\alpha^2)/(\mu\alpha^2)=(2.0\pm1.2)\times10^{-5}$  and  $\Delta(\mu\alpha^2g_p^{0.64})/(\mu\alpha^2g_p^{0.64})=(-4.7\pm1.9)\times10^{-6}$ .

Atomic spectroscopy; Molecular spectroscopy; Cosmological constant experiments

PACS number(s): .....

Citation: Renzhi Su, et al.,

, Sci. China-Phys. Mech. Astron. xx, 000000 (2025), https://doi.org/xx

### 1 Introduction

The gyro-magnetic ratio of proton  $(g_p)$ , as a fundamental physical constant, is predicted to exhibit temporal variations in theoretical frameworks attempting to unify the Standard Model of Particle Physics with General Relativity [e.g. 1, 2, 3]. Currently, only three observational constraints on  $g_p$  have been obtained toward B0218+357 at z = 0.6846, M31, and PKS 1830-211 at z = 0.8858 [4, 5, 6]. However, these constraints are not stringent with a precision of  $\sim 10^{-3}$ . There are no other tests of the variation of  $g_p$  although various terrestrial experiments and astronomical observations have been carried out [e.g. 7, 8, 9, 10, 11, 12, 13, 14, 15, 16, 17], which have constrained the variations of fine-structure constant,  $\alpha$ , proton-electron mass ratio,  $\mu$ , and combinations of  $\alpha$ ,  $\mu$  and  $g_p$  to precisions of  $\leq 10^{-5}$ , see a recent review by [18].

†Email: rzsu.astro@gmail.com

<sup>\*</sup>These authors contribute equally to this work.

Here we report a constraint on the cosmological variation of  $g_p$  utilizing H I 21 cm and OH 18 cm lines observed with the newly commissioned Five-hundred-meter Aperture Spherical radio Telescope [FAST; 19, 20] toward PKS 1413+135.

PKS 1413+135 is a BL Lac object towards which an optical spiral galaxy was observed at z=0.247 [21]. Various radio absorption lines, arising from the spiral galaxy, have been detected towards the radio source, including atomic H I (21 cm) [22], conjugate OH 18 cm satellite lines [7, 14, 23, 24]<sup>1)</sup> and millimeter band molecular (CO, HNC and HCO<sup>+</sup>) lines [25, 26]. The latter were only seen towards the radio core where there is sufficient high frequency continuum (43 GHz) flux when the H I absorption was detected towards the eastern jet [21, 27]. The most sensitive observation of the OH satellite lines has provided a constraint of  $[\Delta Y/Y] = (-1.0 \pm 1.3) \times 10^{-6}$ , where  $Y \equiv \mu \alpha^2 g_p^{0.54}$  [14], although  $g_p$  was implicitly assumed to be constant which we do not assume here.

#### 2 Observations and data reduction

The observations were carried out on 1st September 2022 with On-Off mode. The observations utilized the FAST L-band 19-beam receiver covering 1.00–1.50 GHz, over 65 536 channels, which gives a beam size of  $\sim$  3 arcmins. The large bandwidth allows us to observe the redshifted H I and four OH lines simultaneously, while retaining a high spectral resolution. The On and Off time was set to 300 s, and 10 On-Off cycles were used with all the 19 beams. To optimize the observing time, we followed the same strategy as [28, 29] – selecting a special Off point for beam 01, so that when the beam was off the source, beam 14 that is about 11.5 arcmins left to beam 01 was on the source. Therefore, both beam 01 and beam 14 were recording data, giving a total on-source time of 6000 s (100 minutes). The data were recorded every 0.1 s, and a noise diode,  $\approx$  12.5 K, were injected for 3  $\times$  90 s to calibrate the flux.

We individually reduced the XX and YY polarization data from each beam and each On-Off cycle. Therefore, each line has 40 On-Off spectra. We first used the noise diode and the gain curves to calibrate the spectral flux. For each On-Off cycle, the Off-target spectrum was then subtracted from the On-target spectrum to calibrate the bandpass. Following this, a combination of a third-degree polynomial and a sine functions was fitted to line-free channels to subtract the continuum.

All four OH 18 cm lines are free of RFI, although for eight (out of 40) of the OH 1720 spectra we could not satisfactorily fit the continuum and so these were not used. Intermittent weak RFI affected four H I spectra, which were also removed from the analysis. A Kolmogorov-Smirnov test on the line-free channels of the remaining spectra showed the noise to be Gaussian and so these were retained. Finally, the spectra for each line were combined, weighted based on their measured root-mean-square (RMS) noise, to produce the final spectra for the individual transitions. Since the OH main lines have relatively low signal-noise-ratio, they were resampled to a frequency resolution of  $\Delta v = 29 \text{ kHz}$  ( $\Delta v = 6.3 \text{ km s}^{-1}$ ), using the Python-based S pectRes [30].

### 3 Spectra and redshift measurements

We show the spectra in Figure 1 and 2. The spectral properties are listed in Table 1. We detected OH 18 cm main lines<sup>2)</sup> toward PKS 1413+135 and they have the same velocity width. The OH 18 cm satellite lines still remain conjugate (Figure 2), compared to previous observations [14].

We fitted the spectra with Gaussian functions. The H  $_{\rm I}$  line has a very high signal-noise-ratio (SNR), with the peak absorption having SNR  $\approx$  1640. The high SNR reveals many subtle structures beyond the scope of our phenomenological model. The H  $_{\rm I}$  line of PKS 1413+135 was observed with GBT telescope as well, which was well fitted with four components [7]. In principle, we can directly use the GBT spectrum to conduct our studies. However, using our FAST H  $_{\rm I}$  spectrum can avoid some systematic uncertainties. Note that in our H  $_{\rm I}$  line fitting practice we consistently identify a component matching the deep absorption structure whose full width at half-maximum (FWHM) is consistent with the Gaussian functions fitted to the OH 1665 and 1667 MHz lines, which indicates that these lines arise from the same gas cloud and hence we can compare their observed redshifts to measure the evolution of fundamental constants. We further checked the GBT spectrum and found this

<sup>1)</sup> When the pumping is dominated by the intraladder 119 μm transition, the OH 18 cm satellite lines will appear as stimulated absorption (1612 MHz) and emission (1720 MHz) with the same strength, showing conjugate behavior while the OH 18 cm main lines are suppressed, exhibiting no absorption/emission.

<sup>2)</sup> Note that the OH 1667 line was reported to be detected toward PKS 1413+135 more than twenty years ago with Giant Metrewave Radio Telescope (GMRT) observations[31], which was however not supported by the higher sensitive Green Bank Telescope (GBT) observations [7].

component matches the H<sub>I</sub> 1 component in the GBT spectrum [7]. Therefore, we finally fitted our H<sub>I</sub> and OH spectra following the scenario below.

- We deteriorated the sensitivity by manually injecting a noise of 4 mJy into the H<sub>I</sub> spectrum, which effectively downweights the overconstrained regions while preserving the overall profile shape. This method has been used to fit the H<sub>I</sub> spectrum of M31 [5]. After injecting the 4 mJy noise, we found that our H<sub>I</sub> spectrum can be fitted with four components that are consistent with the components fitted to the GBT H<sub>I</sub> line, which demonstrates the feasibility and reliability of our method of injecting extra noise.
- Four Gaussian components, named as H<sub>I</sub>-g<sub>1</sub>, H<sub>I</sub>-g<sub>2</sub>, H<sub>I</sub>-g<sub>3</sub> and H<sub>I</sub>-g<sub>4</sub>, were fitted to our H<sub>I</sub> spectrum while each OH spectrum was fitted with one Gaussian component.
- The FWHMs of H<sub>I</sub>-g1, OH 1665, and OH 1667 MHz lines were tied to be the same. Here, the H<sub>I</sub>-g1 was used to represent the deep H<sub>I</sub> absorption structure.
- Given the conjugate nature of the OH satellite lines, their FWHMs were tied to be the same and their amplitudes were set to be opposite.
- To obtain the statistical uncertainties, we conducted a Monte Carlo simulation. We repeated the fits for 10,000 times. Each time, we added Gaussian random noises, characterized by the noise values of H<sub>I</sub> and OH spectra, to the best fitted models of H<sub>I</sub> and OH lines, respectively. We used the averages as the best fitted parameters and the standard deviations as associated uncertainties.

The best fitted parameters and their associated uncertainties are listed in Table 1. The simultaneous fit of H I and OH main lines gave a  $\chi^2_{\text{red}} = 1.04 \pm 0.10$  while the simultaneous fit of OH satellite lines gave a  $\chi^2_{\text{red}} = 1.02 \pm 0.06$ , reflecting a good fit.

When measuring the redshifts, the laboratory frequencies,  $v_{\text{H I}} = 1420.405751768(2)$  MHz,  $v_{1612} = 1612.230825(15)$  MHz,  $v_{1665} = 1665.401803(12)$  MHz,  $v_{1667} = 1667.358996(4)$  MHz,  $v_{1720} = 1720.529887(10)$  MHz, were used [32, 33, 34].

# 4 Systematic errors

Any uncertainties and potential errors would influence the results and thus should be identified. The uncertainties can be classified as statistical and systematic. The former has been determined from the Monte Carlo simulation. The latter cloud arise from a catalog including Earth's motion, frequency calibration, errors in the laboratory frequencies, radio frequency interference (RFI), and astronomical errors arising in the target source.

The data were recorded in topocentric frequency without correction for the Earth's motion during the observations, converting the observed frequencies into the barycentric frame in the data reduction. However, we claim that this does not influence our results at all, because H I and OH lines were observed simultaneously. This ensures that any velocity shifts due to observational conditions apply equally to all lines, preserving the relative velocity difference between lines which is the key element in our analysis.

Being phase-locked to a maser radio spectrometers are very stable. The relevant uncertainties are ignorable compared to those caused by the errors of laboratory frequencies. Taking the OH 1665 MHz line as an example, its laboratory frequency is 1665.401803 MHz with an error of 0.000012 MHz. This error can cause an uncertainty of  $2.2 \times 10^{-3}$  km s<sup>-1</sup> in the velocity of OH 1665 MHz line. The systematic uncertainties caused by the laboratory frequencies are listed in Table 1.

Regarding to RFI, all of the OH lines were completely free of this with a minority of the H<sub>I</sub> spectra being mildly affected, which have been removed.

Of the issues arising from source itself, possible effects are the motion of the absorbing gas and variability in the background radio source [24]. However, these variations occur on timescales of years and should not be an issue in the two-hour observation, no matter to mention that the simultaneity of the spectral line observations can ensure that the possible slight uncertainties caused by source itself on the lines can be almost balanced out.

Therefore, the main source of systematic uncertainties is laboratory frequencies in virtue of the simultaneous spectral line observations that canceled out most systematic uncertainties. In comparison, see Table 1, the systematic uncertainties are ignorable compared to the statistical uncertainties.

#### 5 Evolution of fundamental constants

The line frequencies of H<sub>I</sub> 21-cm hyperfine transition and OH 18-cm transitions have the dependencies [4, 35]:

$$\nu_{21} \propto g_p \mu^{-1} \alpha^2 R_{\infty},\tag{1}$$

$$v_{1667} + v_{1665} \propto \mu^{-2.57} \alpha^{-1.14} R_{\infty},$$
 (2)

$$v_{1667} - v_{1665} \propto \mu^{-2.44} \alpha^{-0.88} g_p R_{\infty},$$
 (3)

$$\nu_{1720} - \nu_{1612} \propto \mu^{-0.72} \alpha^{2.56} g_{\nu} R_{\infty},$$
 (4)

where  $R_{\infty} \equiv m_e e^4/(\hbar^3 c)$  is the Rydberg constant. Therefore, the line frequency ratios can provide us the variation of  $\alpha$ ,  $\mu$ , and  $g_p$ . From [4], the comparison of redshifts:

- Between  $v_{1667} + v_{1665}$  and  $v_{1667} - v_{1665}$  gives

$$\frac{\Delta z_1}{1+z_1} = 0.13 \frac{\Delta \mu}{\mu} + 0.26 \frac{\Delta \alpha}{\alpha} + \frac{\Delta g_p}{g_p} = \frac{\Delta (\mu^{0.13} \alpha^{0.26} g_p)}{\mu^{0.13} \alpha^{0.26} g_p},\tag{5}$$

where  $\Delta z_1 = z(\nu_{1667} + \nu_{1665}) - z(\nu_{1667} - \nu_{1665})$  is the difference in the measured  $\nu_{1667} + \nu_{1665}$  and  $\nu_{1667} - \nu_{1665}$  redshifts and  $z_1 = \frac{1}{2} \left[ z(\nu_{1667} + \nu_{1665}) + z(\nu_{1667} - \nu_{1665}) \right]$  is the average.

- Comparison between  $v_{1667} + v_{1665}$  and H<sub>I</sub> gives

$$\frac{\Delta z_2}{1+z_2} = 1.57 \frac{\Delta \mu}{\mu} + 3.14 \frac{\Delta \alpha}{\alpha} + \frac{\Delta g_p}{g_p} = \frac{\Delta (\mu^{1.57} \alpha^{3.14} g_p)}{\mu^{1.57} \alpha^{3.14} g_p},\tag{6}$$

where  $\Delta z_2 = z(\nu_{1667} + \nu_{1665}) - z(\text{Hi}), z_2 = \frac{1}{2} [z(\nu_{1667} + \nu_{1665}) + z(\text{Hi})].$ 

- Between  $v_{1667}$  -  $v_{1665}$  and H<sub>I</sub> gives

$$\frac{\Delta z_3}{1+z_3} = 1.44 \frac{\Delta \mu}{\mu} + 2.88 \frac{\Delta \alpha}{\alpha} = \frac{\Delta(\mu^{1.44} \alpha^{2.88})}{\mu^{1.44} \alpha^{2.88}},\tag{7}$$

where  $\Delta z_3 = z(v_{1667} - v_{1665}) - z(\text{Hi})$  and  $z_3 = \frac{1}{2}[z(v_{1667} - v_{1665}) + z(\text{Hi})].$ 

- Between  $v_{1720} + v_{1612}$  and  $v_{1720} - v_{1612}$  gives

$$\frac{\Delta z_4}{1 + z_4} = 1.85 \frac{\Delta \mu}{\mu} + 3.70 \frac{\Delta \alpha}{\alpha} + \frac{\Delta g_p}{g_p} = \frac{\Delta (\mu^{1.85} \alpha^{3.70} g_p)}{\mu^{1.85} \alpha^{3.70} g_p},\tag{8}$$

where  $\Delta z_4 = z(\nu_{1720} + \nu_{1612}) - z(\nu_{1720} - \nu_{1612})$  and  $z_4 = \frac{1}{2} [z(\nu_{1720} + \nu_{1612}) + z(\nu_{1720} - \nu_{1612})]$ .

Applying these Equations to our data, we obtained the following results. The comparisons between  $v_{1667} + v_{1665}$  and  $v_{1667} - v_{1665}$ , between  $v_{1667} + v_{1665}$  and H I-g1, between  $v_{1667} - v_{1665}$  and H I-g1 separately, give:

Set 1 
$$\begin{cases} \frac{\Delta\mu}{\mu} + 2\frac{\Delta\alpha}{\alpha} + 7.75\frac{\Delta g_p}{g_p} = (0 \pm 4.0) \times 10^{-2} & \text{(a)} \\ \frac{\Delta\mu}{\mu} + 2\frac{\Delta\alpha}{\alpha} + 0.64\frac{\Delta g_p}{g_p} = (-4.7 \pm 1.9) \times 10^{-6} & \text{(b)} \\ \frac{\Delta\mu}{\mu} + 2\frac{\Delta\alpha}{\alpha} = (0 \pm 3.5) \times 10^{-3} & \text{(c)}. \end{cases}$$

From the conjugate OH satellite lines we determine  $[\Delta Y/Y] = (1.5 \pm 5.2) \times 10^{-6}$ . Moreover, we obtain  $[\Delta Y/Y] = (-0.9 \pm 1.3) \times 10^{-6}$ , by combining it with  $[\Delta Y/Y] = (-1.0 \pm 1.3) \times 10^{-6}$  from previous observations [14], weighted based on their uncertainties. Note that  $g_p$  was implicitly assumed to be non-variable [14], which we do not assume here.

Connecting Equation 9(b) to  $[\Delta Y/Y] = (-0.9 \pm 1.3) \times 10^{-6}$ , we further have  $\Delta g_p/g_p = (-4.3 \pm 2.5) \times 10^{-5}$  and  $\Delta(\mu\alpha^2)/(\mu\alpha^2) = (2.0 \pm 1.2) \times 10^{-5}$ .

## 6 Summary

-From the FAST observations of H<sub>I</sub> and OH spectral lines toward PKS 1413+135, a stringent constraint,  $\Delta g_p/g_p = (-4.3 \pm 2.5) \times 10^{-5}$ , is placed on the cosmological variation of the proton g-factor over a look-back time of 2.9 Gyr. In addition, we obtained  $\Delta(\mu\alpha^2)/(\mu\alpha^2) = (2.0 \pm 1.2) \times 10^{-5}$  and  $\Delta(\mu\alpha^2g_p^{0.64})/(\mu\alpha^2g_p^{0.64}) = (-4.7 \pm 1.9) \times 10^{-6}$ . These are consistent with no evolution. Compared to previous constraints on  $g_p$  [4, 5, 6], our result improves the constraint by more than two orders of magnitude. With the FAST, and the future Square Kilometre Array (SKA), we expect further high quality detections [35, 36], leading to experimental constraints on current grand unified theories of physics.

## 7 Acknowledgements

This work is supported by the National Natural Science Foundation of China (Grant No. 12588202). RZS acknowledges the support from the China Postdoctoral Science Foundation (Grant No. 2024M752979). MFG is supported by the National Science Foundation of China (grant 12473019), the Shanghai Pilot Program for Basic Research-Chinese Academy of Science, Shanghai Branch (JCYJ-SHFY-2021-013), the National SKA Program of China (Grant No. 2022SKA0120102), and the China Manned Space Project with No. CMS-CSST-2025-A07.

This work made use of the data from FAST (Five-hundred-meter Aperture Spherical radio Telescope). FAST is a Chinese national mega-science facility, operated by National Astronomical Observatories, Chinese Academy of Sciences.

## 8 Conflict of interest

The authors declare no competing interests.

## 9 Data availability

The raw data has been released by the FAST. The final spectra are available here (https://github.com/SURENZHI/FAST-HI-and-OH-spectra-of-PKS-1413-135).

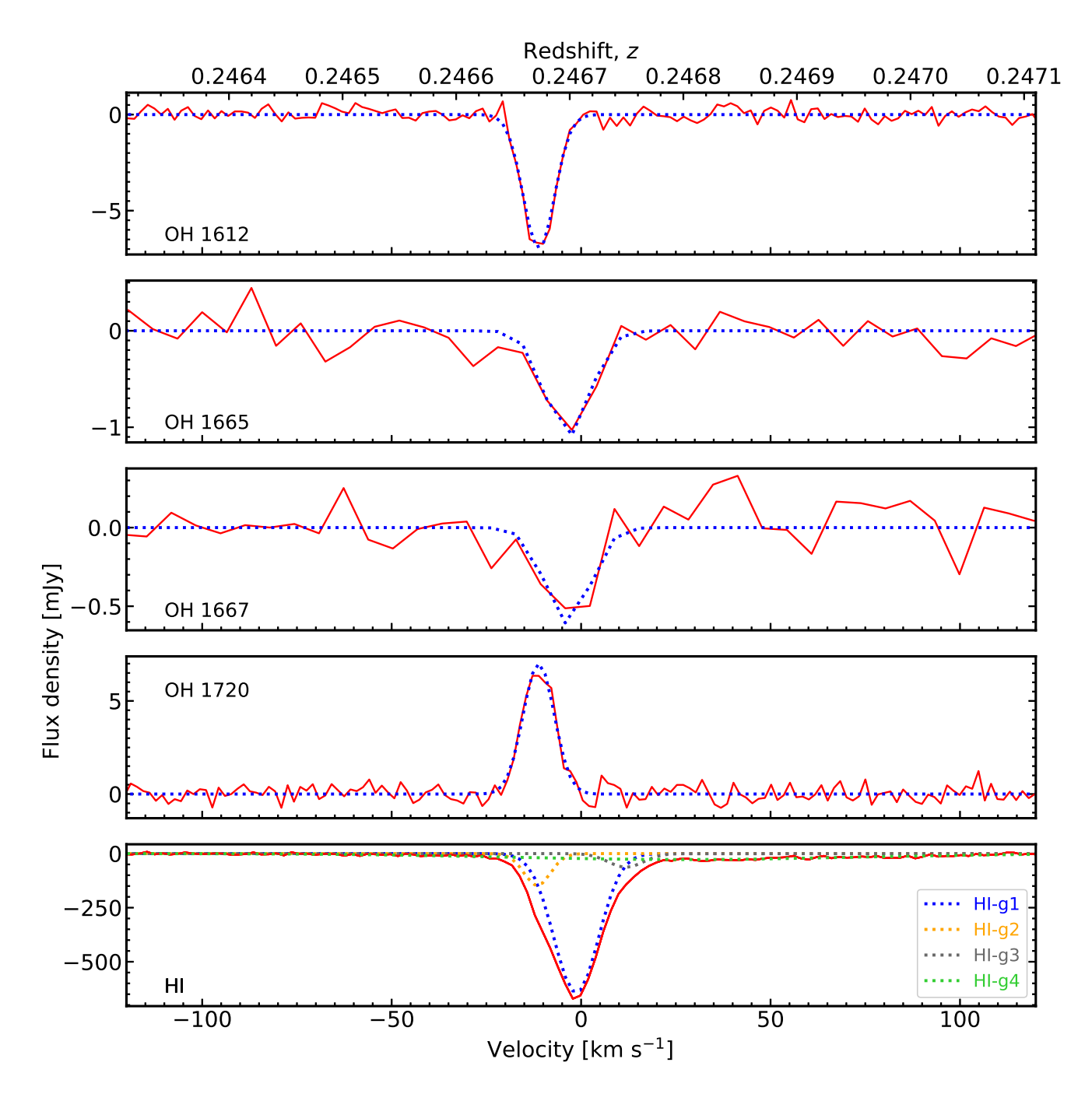
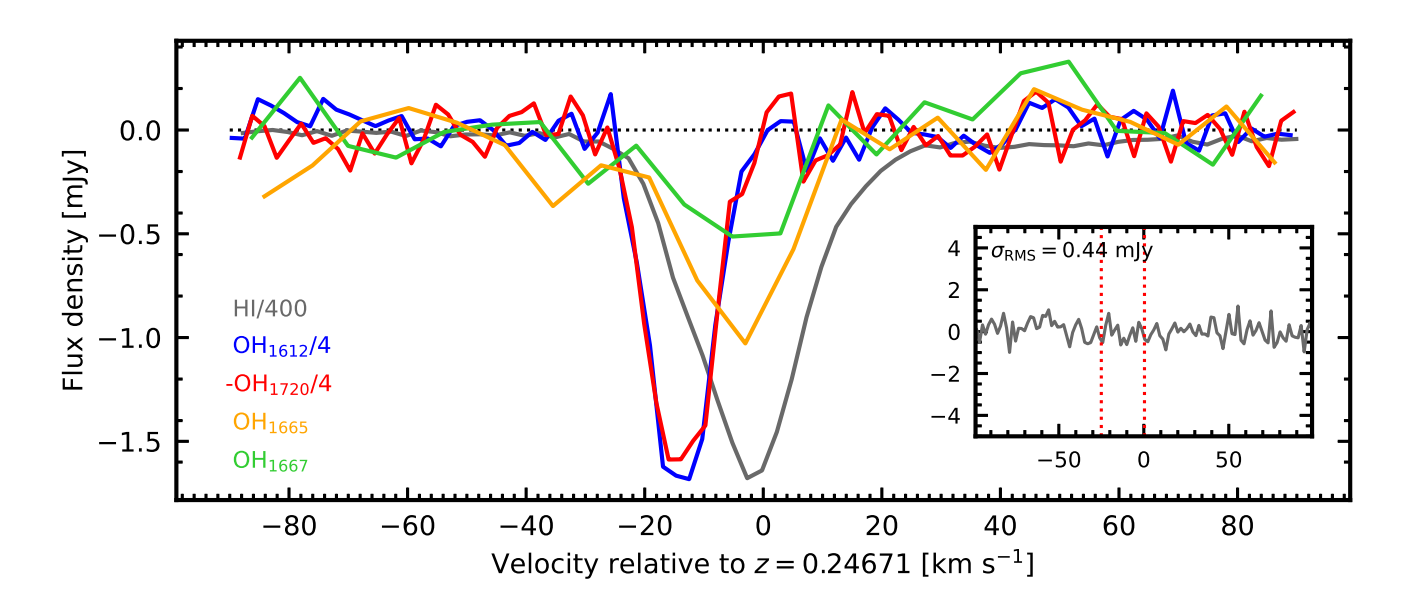


Figure 1 The FAST H<sub>1</sub> and OH spectra in the source rest frame with respect to z = 0.24671. The dotted lines show the Gaussian fits. While the OH lines are fitted with single Gaussian profile, the H<sub>1</sub> line is best fit with four, labeled as H<sub>1</sub>-g<sub>1</sub>, H<sub>1</sub>-g<sub>2</sub>, H<sub>1</sub>-g<sub>3</sub> and H<sub>1</sub>-g<sub>4</sub> with decreasing peak absorption.

The measured properties of absorption lines towards PKS 1413+135. The columns are the transition, the peak absorption flux density, FWHM, velocity with respect to z = 0.24671, statistical Table 1

uncertainties of	uncertainties of the velocity, systematic uncertainties	tic uncertainties of	f the velocity, 1	neasured re	dshift, spectral re	of the velocity, measured redshift, spectral resolution, and the RMS noise.			
Line	$S_{ m peak}$	FWHM	Velocity E <sub>stas</sub>	$\mathbf{E}_{ ext{stas}}$	$\mathrm{E}_{\mathrm{sys}}$	2	$\Delta v$	$\sigma_{ extsf{RMS}}$	
	$mJy beam^{-1}$	${\rm kms^{-1}}$	$\mathrm{km}\mathrm{s}^{-1}$ $\mathrm{km}\mathrm{s}^{-1}$	${\rm kms^{-1}}$	${\rm kms^{-1}}$		${\rm kms^{-1}}$	${\rm kms^{-1}}$ mJy beam <sup>-1</sup>	
Hr-g1	$-626.7 \pm 49.3$	$13.7 \pm 0.8$	-1.36	0.16	$4.2 \times 10^{-7}$	$0.24670434 \pm 6.7 \times 10^{-7}$	2.0	4.00	
Hr-g2	$-150.8 \pm 23.3$	$8.3 \pm 0.5$	-11.52	0.36	$4.2 \times 10^{-7}$	$0.2466621 \pm 1.5 \times 10^{-6}$	2.0	4.00	
Hr-g3	$-77.5 \pm 41.5$	$11.4 \pm 2.5$	10.99	2.66	$4.2 \times 10^{-7}$	$0.246756 \pm 1.1 \times 10^{-5}$	2.0	4.00	
Hr-g4	$-27.6 \pm 1.1$	$107.3 \pm 3.7$	27.78	1.88	$4.2 \times 10^{-7}$	$0.2468255 \pm 7.8 \times 10^{-6}$	2.0	4.00	
OH 1612	$-7.0 \pm 0.1$	$9.7 \pm 0.2$	-11.14	0.12	$2.8\times10^{-3}$	$0.24666367 \pm 5.0 \times 10^{-7}$	1.8	0.29	
OH 1665	$-1.1\pm0.1$	$13.7 \pm 0.8$	-3.52	1.03	$2.2\times10^{-3}$	$0.2466953 \pm 4.3 \times 10^{-6}$	6.5	0.16	
OH 1667	$-0.6 \pm 0.1$	$13.7 \pm 0.8$	-3.56	1.4	$7.2 \times 10^{-4}$	$0.2466952 \pm 6.0 \times 10^{-6}$	6.5	0.13	
OH 1720	$7.0 \pm 0.1$	$9.7 \pm 0.2$	-11.19	0.15	$1.7\times10^{-3}$	$0.24666346 \pm 6.2 \times 10^{-7}$	1.7	0.36	



**Figure 2** Overlay of the H I and OH spectra shifted to the source rest frame. The strength of 1612, 1720 and H I lines are divided by a factor of 4, -4 and 400, respectively. The inset shows the sum of the 1612 and 1720 lines, with the red vertical lines marking the range of the absorption which is consistent with the noise, as expected from the conjugate nature.

#### References

- 1 W. J. Marciano, Time variation of the fundamental 'constants' and Kaluza-Klein theories, Phys. Rev. Lett. 52 (1984) 489–491. doi:10.1103/PhysRevLett.52.489.
- 2 T. Damour, A. M. Polyakov, The string dilation and a least coupling principle, Nuclear Physics B 423 (2-3) (1994) 532–558. arXiv:hep-th/9401069, doi:10.1016/0550-3213(94)90143-0.
- 3 L.-X. Li, I. Gott, J. Richard, Inflation in Kaluza-Klein theory: Relation between the fine-structure constant and the cosmological constant, Phys. Rev. D 58 (10) (1998) 103513. arXiv:astro-ph/9804311, doi:10.1103/PhysRevD.58. 103513.
- 4 J. N. Chengalur, N. Kanekar, Constraining the Variation of Fundamental Constants using 18cm OH Lines, Phys. Rev. Lett. 91 (24) (2003) 241302. arXiv:astro-ph/0310764, doi:10.1103/PhysRevLett.91.241302.
- 5 R. Su, T. An, S. J. Curran, M. P. Busch, M. Gu, D. Li, Constraints on the Fractional Changes of the Fundamental Constants at a Look-back Time of 2.5 Myr, Astrophys. J. Lett. 981 (2) (2025) L25. arXiv:2502.14576, doi:10.3847/2041-8213/adb843.
- 6 R. Su, S. J. Curran, F. Combes, N. Gupta, S. Muller, D. Li, M. Gu, New constraints on the values of the fundamental constants at a look-back time of 7.3 Gyr, arXiv e-prints (2025) arXiv:2505.07200arXiv:2505.07200, doi:10.48550/arXiv.2505.07200.
- 7 J. Darling, A Laboratory for Constraining Cosmic Evolution of the Fine-Structure Constant: Conjugate 18 Centimeter OH Lines toward PKS 1413+135 at z = 0.24671, Astrophys. J. 612 (1) (2004) 58–63. arXiv:astro-ph/0405240, doi: 10.1086/422450.
- 8 T. Rosenband, D. B. Hume, P. O. Schmidt, C. W. Chou, A. Brusch, L. Lorini, W. H. Oskay, R. E. Drullinger, T. M. Fortier, J. E. Stalnaker, S. A. Diddams, W. C. Swann, N. R. Newbury, W. M. Itano, D. J. Wineland, J. C. Bergquist, Frequency Ratio of Al<sup>+</sup> and Hg<sup>+</sup> Single-Ion Optical Clocks; Metrology at the 17th Decimal Place, Science 319 (5871) (2008) 1808. doi:10.1126/science.1154622.
- 9 M. T. Murphy, V. V. Flambaum, S. Muller, C. Henkel, Strong Limit on a Variable Proton-to-Electron Mass Ratio from Molecules in the Distant Universe, Science 320 (5883) (2008) 1611. arXiv:0806.3081, doi:10.1126/science. 1156352.
- 10 S. J. Curran, A. Tanna, F. E. Koch, J. C. Berengut, J. K. Webb, A. A. Stark, V. V. Flambaum, Measuring space-time variation of the fundamental constants with redshifted submillimetre transitions of neutral carbon, Astron. Astrophys. 533 (2011) A55. arXiv:1108.0976, doi:10.1051/0004-6361/201117457.
- 11 J. A. King, J. K. Webb, M. T. Murphy, V. V. Flambaum, R. F. Carswell, M. B. Bainbridge, M. R. Wilczynska, F. E. Koch, Spatial variation in the fine-structure constant new results from VLT/UVES, Mon. Not. R. Astron. Soc. 422 (4) (2012) 3370–3414. arXiv:1202.4758, doi:10.1111/j.1365-2966.2012.20852.x.
- 12 M. S. Onegin, M. S. Yudkevich, E. A. Gomin, Investigation of the Fundamental Constants Stability Based on the Reactor Oklo Burn-Up Analysis, Modern Physics Letters A 27 (40) (2012) 1250232. arXiv:1010.6299, doi:10.1142/S021773231250232X.
- 13 J. Bagdonaite, P. Jansen, C. Henkel, H. L. Bethlem, K. M. Menten, W. Ubachs, A Stringent Limit on a Drifting Protonto-Electron Mass Ratio from Alcohol in the Early Universe, Science 339 (6115) (2013) 46. doi:10.1126/science. 1224898.
- 14 N. Kanekar, T. Ghosh, J. N. Chengalur, Stringent Constraints on Fundamental Constant Evolution Using Conjugate 18 cm Satellite OH Lines, Phys. Rev. Lett. 120 (6) (2018) 061302. arXiv:1801.07688, doi:10.1103/PhysRevLett.120.061302.

- M. Filzinger, S. Dörscher, R. Lange, J. Klose, M. Steinel, E. Benkler, E. Peik, C. Lisdat, N. Huntemann, Improved Limits on the Coupling of Ultralight Bosonic Dark Matter to Photons from Optical Atomic Clock Comparisons, Phys. Rev. Lett. 130 (25) (2023) 253001. arXiv:2301.03433, doi:10.1103/PhysRevLett.130.253001.
- 16 L. Jiang, Z. Pan, J. N. Aguilar, S. Ahlen, R. Blum, D. Brooks, T. Claybaugh, A. de la Macorra, A. Dey, P. Doel, K. Fanning, S. Ferraro, J. E. Forero-Romero, E. Gaztañaga, S. Gontcho A Gontcho, G. Gutierrez, K. Honscheid, S. Juneau, M. Landriau, L. Le Guillou, M. Levi, M. Manera, R. Miquel, J. Moustakas, E.-M. Mueller, A. Muñoz-Gutiérrez, A. Myers, J. Nie, G. Niz, C. Poppett, F. Prada, M. Rezaie, G. Rossi, E. Sanchez, E. Schlafly, M. Schubnell, H.-J. Seo, D. Sprayberry, G. Tarlé, B. A. Weaver, H. Zou, The DESI Collaboration, Constraints on the Spacetime Variation of the Fine-structure Constant Using DESI Emission-line Galaxies, Astrophys. J. 968 (2) (2024) 120. arXiv:2404.03123, doi:10.3847/1538-4357/ad47b4.
- 17 J.-N. Wei, R.-J. Chen, J.-J. Wei, M. López-Corredoira, X.-F. Wu, Measuring the Time Variation of the Fine-structure Constant with Quasars Detected by LAMOST, Research in Astronomy and Astrophysics 24 (12) (2024) 125021. arXiv: 2409.01554, doi:10.1088/1674-4527/ad9654.
- 18 J.-P. Uzan, Fundamental constants: from measurement to the universe, a window on gravitation and cosmology, arXiv e-prints (2024) arXiv:2410.07281arXiv:2410.07281, doi:10.48550/arXiv.2410.07281.
- 19 R. Nan, D. Li, C. Jin, Q. Wang, L. Zhu, W. Zhu, H. Zhang, Y. Yue, L. Qian, The Five-Hundred Aperture Spherical Radio Telescope (fast) Project, International Journal of Modern Physics D 20 (6) (2011) 989–1024. arXiv:1105.3794, doi:10.1142/S0218271811019335.
- 20 D. Li, P. Wang, L. Qian, M. Krco, P. Jiang, Y. Yue, C. Jin, Y. Zhu, Z. Pan, R. Nan, A. Dunning, FAST in Space: Considerations for a Multibeam, Multipurpose Survey Using China's 500-m Aperture Spherical Radio Telescope (FAST), IEEE Microwave Magazine 19 (3) (2018) 112–119. arXiv:1802.03709, doi:10.1109/MMM.2018.2802178.
- 21 E. S. Perlman, J. T. Stocke, C. L. Carilli, M. Sugiho, M. Tashiro, G. Madejski, Q. D. Wang, J. Conway, The Apparent Host Galaxy of PKS 1413+135: Hubble Space Telescope, ASCA, and Very Long Baseline Array Observations, Astron. J. 124 (5) (2002) 2401–2412. arXiv:astro-ph/0208167, doi:10.1086/344109.
- 22 C. L. Carilli, E. S. Perlman, J. T. Stocke, Discovery of Neutral Hydrogen 21 Centimeter Absorption at Redshift 0.25 toward PKS 1413+135, Astrophys. J. Lett. 400 (1992) L13. doi:10.1086/186637.
- 23 N. Kanekar, J. N. Chengalur, T. Ghosh, Probing Fundamental Constant Evolution with Redshifted Conjugate-satellite OH Lines, Astrophys. J. Lett. 716 (1) (2010) L23–L26. arXiv:1004.5383, doi:10.1088/2041-8205/716/1/L23.
- 24 F. Combes, N. Gupta, S. Muller, S. Balashev, P. P. Deka, K. L. Emig, H. R. Klöckner, D. Klutse, K. Knowles, A. Mohapatra, E. Momjian, P. Noterdaeme, P. Petitjean, P. Salas, R. Srianand, J. D. Wagenveld, PKS 1413+135: OH and H I at z = 0.247 with MeerKAT, Astron. Astrophys. 671 (2023) A43. arXiv:2211.09355, doi:10.1051/0004-6361/202245482.
- 25 T. Wiklind, F. Combes, First detection of CO(J=0-¿1) absorption at cosmological distances (z=0.247), Astron. Astrophys. 286 (1994) L9–L12.
- 26 T. Wiklind, F. Combes, Molecular absorption lines at high redshift: PKS 1413+135 (z=0.247), Astron. Astrophys. 328 (1997) 48–68. arXiv:astro-ph/9708051, doi:10.48550/arXiv.astro-ph/9708051.
- 27 C. L. Carilli, K. M. Menten, J. T. Stocke, E. Perlman, R. Vermeulen, F. Briggs, A. G. de Bruyn, J. Conway, C. P. Moore, Astronomical Constraints on the Cosmic Evolution of the Fine Structure Constant and Possible Quantum Dimensions, Phys. Rev. Lett. 85 (26) (2000) 5511–5514. arXiv:astro-ph/0010361, doi:10.1103/PhysRevLett.85.5511.
- 28 Z. Zheng, D. Li, E. M. Sadler, J. R. Allison, N. Tang, A pilot search for extragalactic OH absorption with FAST, Mon. Not. R. Astron. Soc. 499 (3) (2020) 3085–3093. arXiv:2010.01769, doi:10.1093/mnras/staa3033.
- 29 R. Su, M. Gu, S. J. Curran, E. K. Mahony, N. Tang, J. R. Allison, D. Li, M. Zhu, J. N. H. S. Aditya, H. Yoon, Z. Zheng, Z. Wu, FAST Discovery of a Fast Neutral Hydrogen Outflow, Astrophys. J. Lett. 956 (1) (2023) L28. arXiv:2309.01890, doi:10.3847/2041-8213/acf4fa.

- 30 A. C. Carnall, SpectRes: A Fast Spectral Resampling Tool in Python, arXiv e-prints (2017) arXiv:1705.05165arXiv: 1705.05165, doi:10.48550/arXiv.1705.05165.
- 31 N. Kanekar, J. N. Chengalur, Molecular gas at intermediate redshifts, Astron. Astrophys. 381 (2002) L73–L76. arXiv: astro-ph/0111563, doi:10.1051/0004-6361:20011697.
- 32 H. Hellwig, R. F. C. Vessot, M. W. Levine, P. W. Zitzewitz, D. W. Allan, D. J. Glaze, Measurement of the Unperturbed Hydrogen Hyperfine Transition Frequency, IEEE Transactions on Instrumentation Measurement 19 (4) (1970) 200–209. doi:10.1109/TIM.1970.4313902.
- 33 E. R. Hudson, H. J. Lewandowski, B. C. Sawyer, J. Ye, Cold Molecule Spectroscopy for Constraining the Evolution of the Fine Structure Constant, Phys. Rev. Lett. 96 (14) (2006) 143004. arXiv:physics/0601054, doi:10.1103/PhysRevLett.96.143004.
- 34 B. L. Lev, E. R. Meyer, E. R. Hudson, B. C. Sawyer, J. L. Bohn, J. Ye, OH hyperfine ground state: From precision measurement to molecular qubits, Phys. Rev. A 74 (6) (2006) 061402. arXiv:physics/0608194, doi:10.1103/PhysRevA. 74.061402.
- S. J. Curran, N. Kanekar, J. K. Darling, Measuring changes in the fundamental constants with redshifted radio absorption lines, new. a.. r 48 (11-12) (2004) 1095–1105. arXiv:astro-ph/0409141, doi:10.1016/j.newar.2004.09.004.
- 36 X. Chen, S. P. Ellingsen, Y. Mei, Astrophysical constraints on the proton-to-electron mass ratio with FAST, Research in Astronomy and Astrophysics 19 (2) (2019) 018. arXiv:1904.03871, doi:10.1088/1674-4527/19/2/18.